

White Paper XXIII

Some Electric/Magnetic Aspects of Space Conditioning Via the Use of an Intention-Host Device

by

William A Tiller, Ph.D. and Walter E. Dibble, Jr., Ph.D.

Introduction

For the past dozen years or so, the authors have been investigating the “conditioning” of various experimental spaces using an IHD (intention host device) of a particular type⁽¹⁻⁶⁾. This space conditioning actually changes the electromagnetic (EM) gauge symmetry state of the experimental space⁽⁷⁾ which, in turn, allows human intention, via the use of this type of an IHD, to significantly change the properties of materials. Two very recent publications by us appears to have renewed many readers’ interest in this topic because the space can, in principle, be sustained at a certain **excess** thermodynamic free energy level of “conditioning” for long periods of time and, in fact, the specific intentions can be broadcast over long distances and replicated elsewhere⁽⁸⁾. We now wish to share some of our understanding of the electric and magnetic aspects of such a device. It is important to add that this device appears to function at two uniquely different levels of physical reality, (1) our conventional distance-time level, labeled the D-space level, our normal U(1) gauge symmetry state materials level and (2) our subtle domains, vacuum level, labeled the R-space (or reciprocal) level, of higher SU(2) gauge symmetry state materials level⁽⁶⁾. In a “conditioned” space, what is usually created is some volume fraction of SU(2) material within a matrix of U(1) material. It is interesting to note that competent electrical engineers will look at the circuit diagram for this IHD⁽⁹⁾ and state that it cannot possibly work! This is quite true from a D-space **only** perspective but seemingly not true from such a duplex-space perspective!

Some Theoretical/Experimental Background on pH-meters

The majority of our experimental studies have been carried out using sensors of the pH-meter, thermometer and thermistor types. Although the readouts of these digital instruments are chemical activity of the H⁺-ion and temperature, respectively, they are primarily a digital electrical measurement involving changes in electric voltage and electric current as a function of time. Let us focus our attention on the pH-sensor but begin with a brief primer on thermodynamics.

Thermodynamics is thought to be the master area of scientific enquiry that ultimately governs all processes in nature, whether in our conventional U(1) EM gauge symmetry state spaces or in higher gauge symmetry state spaces. In visual experience, it looks like they occupy the identical volume of space but some of its unseen structure and qualities are different. For us, we are particularly interested in the U(1) and the SU(2) gauge states⁽¹⁰⁾. In the U(1) state, Maxwell's equations of EM apply exactly; however, in the SU(2) state, Maxwell's equations must be modified.

In thermodynamics, one of the most important quantities is the Gibbs free energy per unit volume, G , of a material and it varies in magnitude with pressure, P , temperature, T , and chemical concentration, C , as its main variables. Secondary variables are electric, magnetic, gravitational and other types of fields which can also confer property anisotropy to a material. A very important derivative quantity to G is, for neutral chemical species, called the chemical potential, μ_j , for the j th species and the electrochemical potential, η_j , for ionized species. These have the following relationship to G , i.e.,

(1a)

And

$$G = \sum_j n_j \eta_j + \Delta\mu_j \quad \text{where } \eta = \mu + zeV; \text{ all charged} \quad (1b)$$

Here, n is number per unit volume (same volume as G), μ_0 is the standard state value (one atmosphere and 273° Kelvin) k_B is Boltzmann's constant, T =Temperature, a = chemical activity = γc , (γ =activity coefficient, c =concentration), V =Voltage, e =electric charge, z =charge valence and

$$\Delta\mu_j = \frac{-\hat{v}_j}{2} \frac{d}{dc_j} \left(\varepsilon \underline{E}^2 + m \underline{H}^2 \right) \quad (1c)$$

with \hat{v}_j = molal volume of j, ϵ =electric permittivity of the medium (\underline{E} =electric field in volts/meter) and μ is its magnetic permeability (\underline{H} =magnetic field in ampere/meter).

All of the above is standard for D-space substances. A complementary set of equations are hypothesized to be available for R-space substances simply by placing a subscript D on every term of Equations (1) and a subscript R on every term of the complementary R-space set of equations.

Ultimately, what this leads to for a duplex RF system is the following

$$G_{\text{DUPLEX}} = G_D + \alpha_{\text{eff}} G_R, \quad (2a)$$

$$\mu_{\text{DUPLEX}} = \mu_{jD} + \alpha_{\text{eff}_j} \mu_{jR}, \quad (2b)$$

$$\eta_{\text{DUPLEX}} = \eta_{jD} + \alpha_{\text{eff}_j} \eta_{jR} \quad (2c)$$

and

$$Q_{\text{DUPLEX}} = Q_{Dj} + \alpha_{\text{eff}_j} Q_{Rj} \quad (2d)$$

where, in R-space, magnetic charge and magnetic potential replace the electric charge and electric voltage of D-space.

The U(1) State

With $\alpha_{\text{eff}} \approx 0$, we are dealing with our normal, uncoupled physical reality, the U(1) EM gauge symmetry state⁽⁶⁾ and we will start there to unfold the meaningful considerations in a theoretical assessment of pH-measurement.

The physical aspect of pH measurement involves a device that connects (1) a unit H^+ activity standard chemical cell to (2) an aqueous solution vessel whose H^+ activity, a_{H^+} , is to be measured ($pH = \log_{10}(a_{H^+})$) via (3) an H^+ -permeable membrane located between 1 and 2. As the mobile H^+ -ion redistributes itself in this system to produce electrochemical potential, η_{H^+} , equilibrium (via Equation 1b, $\eta_{H^+} = \text{constant}$) throughout the system so that the H^+ -ion distribution c_{H^+} , changes its spatial profile.

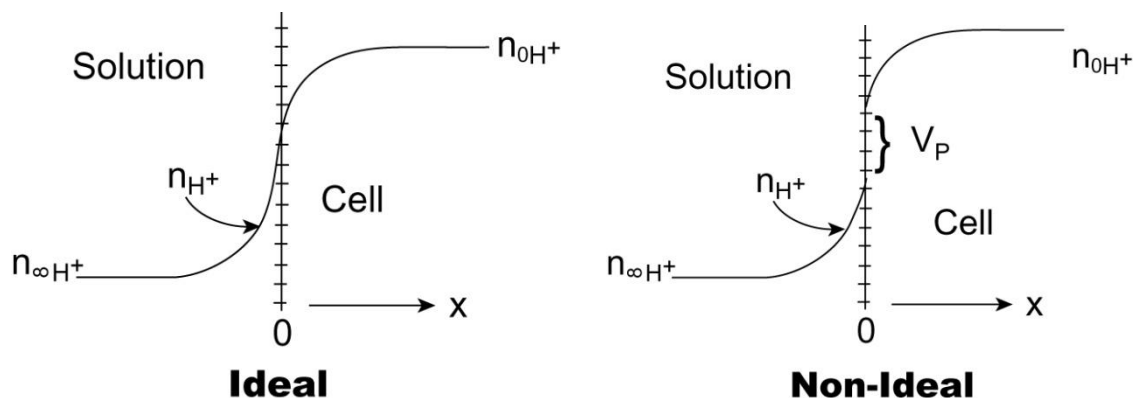


Figure 1. Plots of H^+ ion density, n_{H^+} , profiles in a pH-electrode for (a) the ideal case and (b) the non-ideal case. The theoretically calculated result is qualitatively given by Figures 1 with (1a) and (1b) being for the ideal case and the non-ideal case, respectively.

Utilizing Equation 1b and Figures 1, the thermodynamic equilibrium process for the very mobile H^+ -ions is given by the general Boltzmann equilibrium equation for H^+ , i.e.,

$$\frac{a_{H^+}}{a_{0H^+}} = \exp \left[\frac{-|e|}{k_B T} \{ V - (V_0 + V_p) \} \right] \quad (3a)$$

Here, V_0 is the electric voltage of the standard chemical cell re Figure 1a. $V_p = 0$ in the ideal case but is most generally non-zero and is the interface polarization voltage (Figure 1b) because of redistribution of all other chemical species in the solution. V is the solution voltage, V_0 is the cell voltage, a_0 is the chemical activity for the standard cell, $|e|$ is the proton charge, $|e|/2.303 k_B T = 59.61$ millivolts and T =Temperature. With $a_{0H^+}=1$ and $V_p = 0$, Equation 3a leads to

$$V = V_0 - 59.61 \text{ pH} \text{ mV} \quad (3b)$$

For the **non ideal** or real pH-electrode case with $V_p \neq 0$, a commercial pH-meter's CPU incorporates a corrected temperature factor and utilizes the following parametric expression to **display** the pH from an internal measurement of V_p .

$$V = S \left(\text{pH}_{U(1)} - 7 \right) T_{corr} \quad ; \quad T_{corr} = \frac{T + 273.15}{298.15} \quad (3c)$$

Here, S is the electrode slope $= d[V - (V_0 + V_p)]/d_{pH}$ and $pH = pH_{CPU} = pH_{U(1)}$. In addition, V_0 is taken to be $-7S$ because the experimental isopotential point, $V = 0$ is found to occur at $pH = 7$ for an ideal electrode. In order to make these parametric choices of the commercial pH-electrode, suppliers fit the fundamental physics implicit in Equation 3a. The following is also required for internal self-consistency

$$V_p = (S + 59.16) pH_{U(1)} T_{corr} \quad (3d)$$

Departing From the U(1) State:

Let us take Equation 3c, divide both sides by V , change $pH_{U(1)}$ to pH and, in doing so, call the left-hand-side N , the **Nernst Parameter**, in honor of that great physical chemist of the 1800's where

$$N = \frac{S}{V} (pH - 7) T_{CORR} \quad (4)$$

For the U(1) state, **N must always be unity!** When N is experimentally found not to be unity then pH in Equation 4 has **departed** from $pH_{U(1)}$ to some degree and α_{eff} in Equations 2 has increased in magnitude from zero (although the sign of Q_R , which is a vector, can be positive or negative via the phase angle).

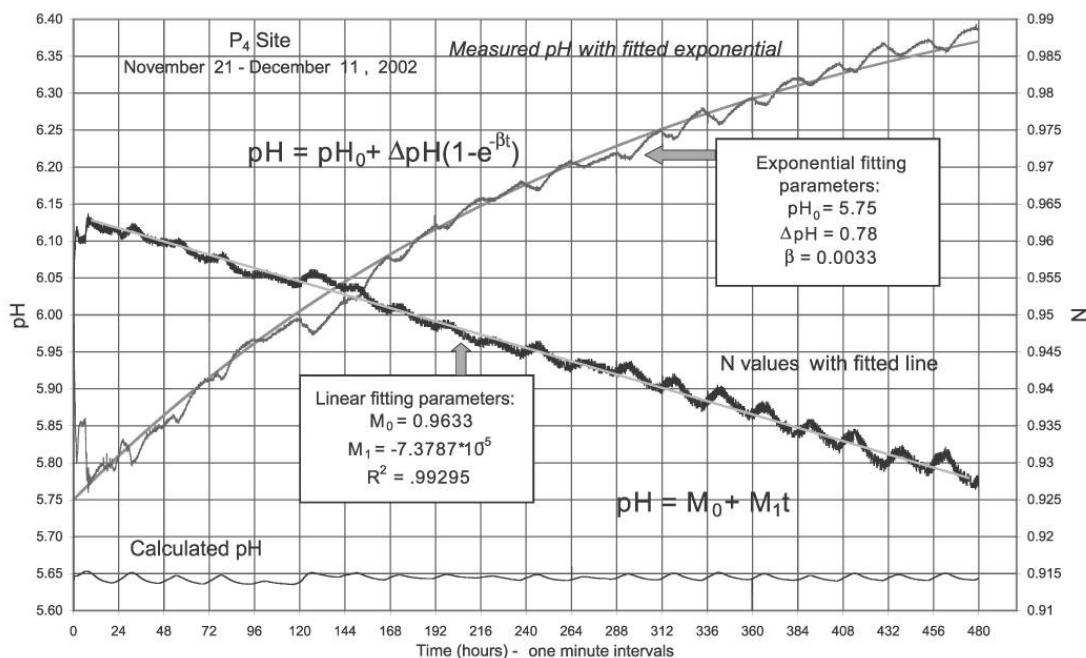


Figure 2. Showing the time-average exponential variation of pH and N after fresh purified water was introduced into the measurement cell on 11/21/02.

Figure 2 illustrates a plot of N-value as a function of time derived from pH-values changing with time. Table 1 shows some 2003 N-values at 8 different experimental sites. This is a very straightforward way for an experimenter to realize that his/her experimental space has become partially conditioned and that the gauge symmetry state is beginning to change to a mixed U(1)/SU(2) state.

Table 1

Values of N for all of the various sites operating in our overall experimental system.

Site	Recent N-values	% departure from 1.00
P ₁	.89	-11
P ₂	1.14	14
P ₃	.98	-2
P ₄	.87	-13
M ₁	1.3	30
K ₁	.98	-2
B ₂	1.23	23
B ₁	1.04	4

In this Table, P=Payson, K=Kansas, M=Missouri, B_A=Baltimore and B_B=Bethesda and the subscript numbers stand for particular measurement stations located at these geographic sites (see Reference 1) as of ~January 25, 2003.

The Mixed SU(2)/U(1) Gauge State

Figure 3 illustrates a linear plot of the general pH-electrode output versus pH_{CPU} meter reading for our normal physical reality (the U(1) state).

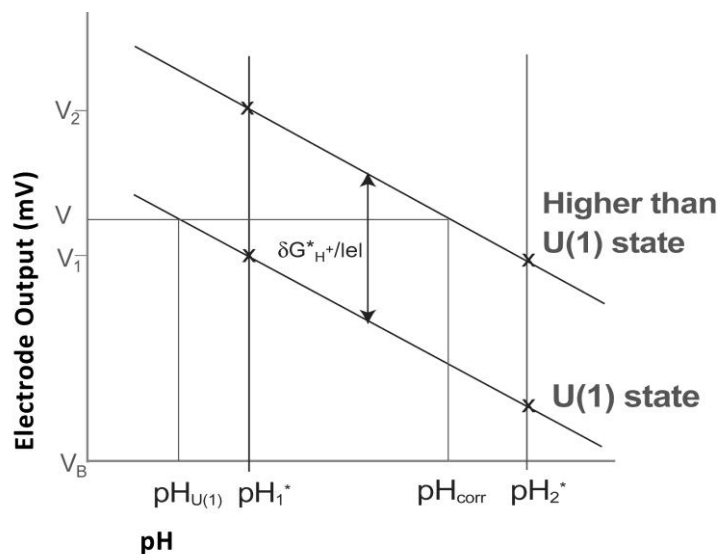


Figure 3. The electrode electrical voltage output vs. pH plots for both the U(1) state ($\delta G^*=0$) and a higher than U(1) EM gauge symmetry state.

The parallel line above it is the absolute value of our hypothesized relationship when some volume fraction, $v_{SU(2)}/v_{U(1)}$, of SU(2) domains have formed within the U(1) matrix of the material being tested. Figure 4 provides a schematic depiction of such a mixture⁽¹¹⁾.

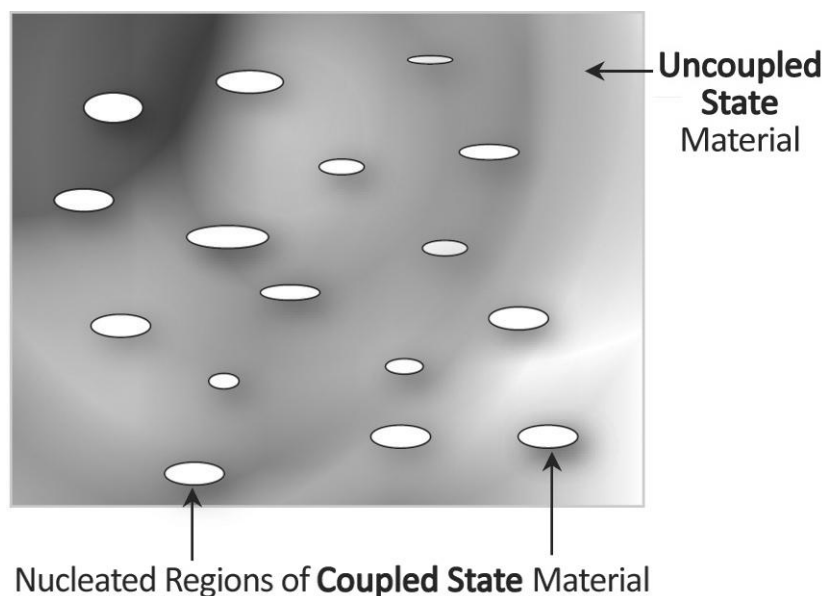


Figure 4. Nucleation and growth of the macroscopic coupled state domains of physical reality.

The presence of the SU(2) domains is thought to both lift the excess thermodynamic free energy state and the pH at constant pH-electrode voltage.

In this case, the analogue to Equation 3a is

$$\frac{a_{H^+}}{a_{0H^+}} = \exp \left[\frac{-|e|}{kT} \left\{ V - (V_o^* + V_P^*) + \frac{\delta G_{H^+}^*}{|e|} \right\} \right] \quad (5a)$$

Now, because H^+ has a magnetic dipole moment due to its spin, and R-space magnetic potential, θ_m , is also present, the standard cell chemical activity, a_{0H^+} , can no longer be assumed to be unity. In addition, V_o^* and V_P^* must be considered to be different from their U(1) EM gauge state values. Thus, taking \log_{10} of both sides of Equation 5a and rearranging, we have

$$V = -59.16 \text{ pH}_{CORR} T_{CORR} + [V_o^* + V_P^* + 59.16 \log_{10} a_{0H^+} - \delta G_{H^+}^* / |e|] \quad (5b)$$

Earlier, it was pedagogically useful to use the parametric form of Equation 3c for expressing the V/pH relationship for the U(1) case. Here, for the mixed SU(2)/U(1) case, our parametric form is chosen to be

$$V = S (pH_{CORR} - 7) T_{CORR} - \delta G_{H^+}^* / |e| \quad (5c)$$

with

$$V_o^* = V_o + \Delta V_{0m} = -7S + \Delta V_{0m},$$

and

$$\left. \begin{aligned} V_P^* &= V_P + \Delta V_{Pm} = (S + 59.16) \text{ pH}_{CORR} - \Delta V_{0m} - 59.16 \log_{10} (a_{0H^+}) \\ \Delta V_{0m} &= (S + 59.16) (pH_{CORR} - pH_{U(1)}) T_{CORR} - \Delta V_{0m} - 59.16 \log_{10} (a_{0H^+}) \end{aligned} \right\} \quad (5d)$$

Using Figure 3 directly, one sees that

$$pH_{CORR} = pH_{U(1)} - \delta G_{H^+}^* / S |e|. \quad (5e)$$

Combining Equations 5c and 5e yields

$$V = S (pH_{U(1)} - 7) T_{CORR} - (1 + T_{CORR}) \frac{\delta G_{H^+}^*}{|e|}. \quad (6a)$$

Since, at the potential point, $V = 0$ and $pH = pH_{U(1)}^0$, Equation 6a becomes

$$\frac{\delta G_{H^+}^*}{|e|} = \frac{S (pH_{U(1)}^0 - 7) T_{CORR}}{1 + T_{CORR}} \quad (6b)$$

So we have gained a quantitative expression for calculating $\delta G_{H^+}^* / |e|$.

Measurement of $pH_{U(1)}^0$ at nine different experimental stations in the Payson laboratory, using the two buffer solutions standard procedure, was carried out via various pH-electrodes (see Figure 5). These were all of the same commercial type but had quite different histories.

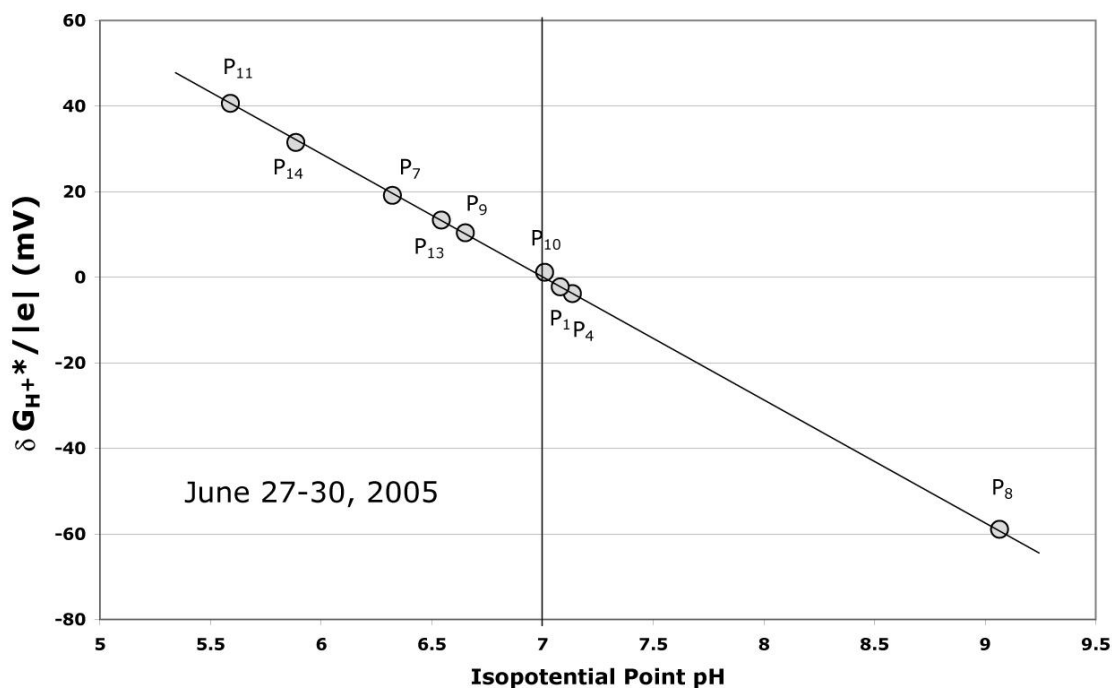


Figure 5. $\delta G_{H^+}^* / |e|$ vs. isopotential point of various electrodes (same type) used at the various P_j stations shown (for the Payson laboratory at calibration). **The only difference between electrodes used at these stations is their history.** The type of space the electrode is exposed to causes the isopotential point to depart from 7.

Our experimental procedure for obtaining $\delta G^*_{H^+}$ at each of these nine sites was to utilize Equation 4 to obtain a value of N for each site, where V and pH_{CORR} are given by Equations 6a and 5e, respectively. When these values of $\delta G^*_{H^+}$ were plotted versus the appropriate values of $pH^0_{U(1)}$, Figure 5 was the result. This is a beautiful linear plot in complete accord with Equation 6b, that yields $\delta G^*_{H^+} = 0$ at $pH^0_{U(1)}$ as expected.

Although $pH_{U(1)}$ is undetermined experimentally, it can always be calculated from standard U(1) state thermodynamics for water in equilibrium with air (T and CO_2 content required). The net result of all this is that, via Equation 6b, we now have a reliable procedure for evaluating, relative to our normal U(1) gauge space, the excess thermodynamic free energy per unit volume of the aqueous H^+ -ion in a particular space that has been partially conditioned via, either an IHD or human biofields. This means that subtle energy experiments, in principle, can now begin to be carried out in meaningfully constant subtle energy environments. Figure 6 illustrates several time-dependent measured values for $\delta G^*_{H^+}$ at different sites P_1 , P_4 , P_5 and P_7 in our Payson, Arizona laboratory.

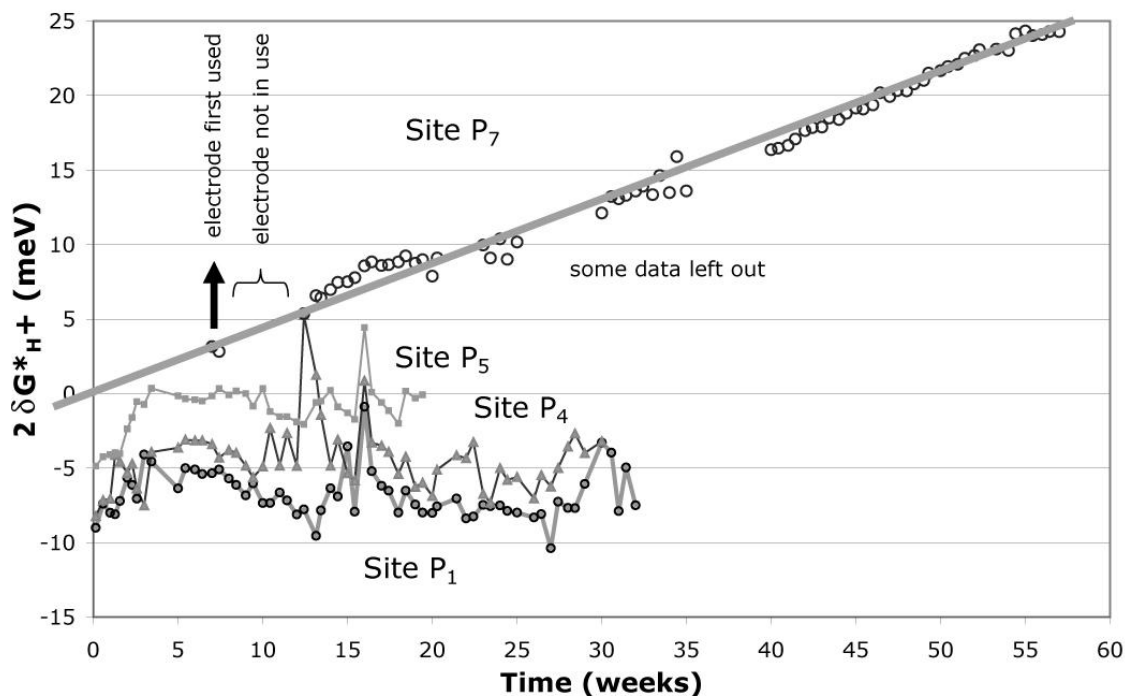


Figure 6. $2\delta G^*_{H^+}$ vs. time plots for four Payson experimental stations.

P₇ is a unique site as it is within a thick, μ -metal vessel, itself within a five-foot cube lined with μ -metal, and manifests a value of $\delta G^*_{H^+} \approx 0.5kT$ after one year. Many other examples of $\delta G^*_{H^+}$ at remote sites (some commercial) were shown in an earlier paper.

Looking at our pH-electrode measurement system at specific locations relative to its larger scale external environment versus to its internal environment, the latter which we have just discussed and come to some meaningful quantitative conclusions, we need to now include the effects associated with **external location** effects on our specific pH-electrode measurements. In addition, we need to recall that, although our sensor output is detailed, time-varying H⁺-ion concentration profiles which also vary somewhat as this sensor is moved from physical location to physical location, the sensor's primary measurement is of an electric voltage nature. Thus, all of today's scientific armament of electrostatics, electrodynamics and electromagnetism need to be taken into consideration when analyzing the results of this experimental work. Ultimately, (1) electrical effects associated with weather changes and earth rotation effects with respect to the sun's radiation field in our external environment are involved. Likewise, (2) internal environmental effects associated with volcanism deep in the earth are involved and (3) the electric continuity equations and the magnetic continuity equations at the earth's surface are meaningfully involved in this category of measurement.

Measurements at a Below-Ground Site and Poisson's Equation

During our replication study of the $\Delta\text{pH} = +1$ unit experiments (2001-2005)⁽³⁾, we learned that significant information entanglement occurred between imprinted IHD-sites and supposed control sites (pH-measurement sites at which no IHD had **ever** been present). In particular, when the control site was under ground, versus at ground level or appreciably above ground, the ΔpH -value increased or decreased significantly from +1 units. Figure 7 illustrates results from such a control site on the C. Norman Shealy M.D., Ph.D., property in Missouri.

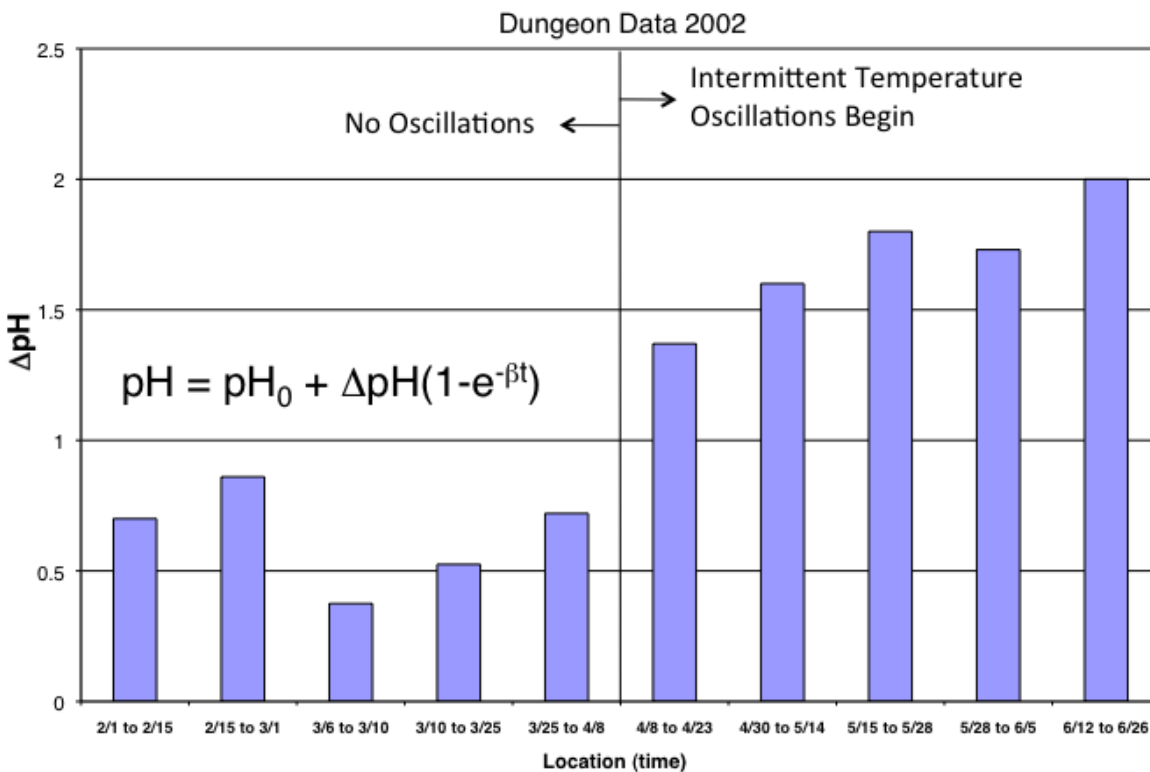


Figure 7. Delta pH as a function of time. Measurements began February 1, 2002. Temperature oscillations only occurred after 2 months of measurement.

$\text{pH} = \text{pH}_0 + \Delta\text{pH}(1 - e^{-\beta t})$					
Location	Date Range	ΔpH -units	$(\text{HR})^{-1}$ Beta	$\Delta\text{pH} \times \text{Beta}$	pH_0
M ₃ : Dungeon	2/1 to 2/15	0.7	0.0039	0.00273	5.755
M ₃ : Dungeon	2/15 to 3/1	0.86	0.0127	0.010922	5.73
M ₃ : Dungeon	3/6 to 3/10	0.375	0.024	0.009	5.72
M ₃ : Dungeon	3/10 to 3/25	0.525	0.0036	0.00189	6.04
M ₃ : Dungeon	3/25 to 4/8	0.72	0.0053	0.003816	5.825
M ₃ : Dungeon	4/8 to 4/23	1.37	0.0045	0.006165	5.90
M ₃ : Dungeon	4/30 to 5/14	1.6	0.0035	0.0056	5.94
M ₃ : Dungeon	5/15 to 5/28	1.8	0.0042	0.00756	5.93
M ₃ : Dungeon	5/28 to 6/5	1.73	0.01	0.0173	5.97
M ₃ : Dungeon	6/12 to 6/26	2	0.008	0.016	5.69

This particular site was labeled “The Dungeon” because it was a small room located about 10 feet underground. Although no IHD had ever been present at the Dungeon site, there were three active IHDs operating elsewhere at that time; one in Missouri about 5 miles away, one in Kansas about 200 miles away and one in Arizona about 1200 miles away. Fresh water and a recalibrated pH-electrode were placed in the water vessel at the Dungeon site to produce a

$$pH_M = pH_0 + \Delta pH (1 - e^{-\beta t}) \quad (7)$$

experimental result for each of these ~2 week time periods. Each of the $(\Delta pH, \beta)$ pair of values is given in Table 1. From this Figure 7/Table 1 data, one clearly sees that (1) substantial and dynamically changing information entanglement is occurring at this particular control site although no active IHD is present so nothing significant is expected to occur and (2) although the three active IHD sites yielded ΔpH -values in the 0.85 to 1.0 range, this underground control site exhibited maximum two week values in the 1.37 to 2.0 range after temperature oscillations (and much less pronounced pH oscillations) began to appear in the data plots.

This Figure 7/Table 1 data presents us with a conundrum consisting of three or four parts:

- (1) In this bar graph, each bar represents ΔpH from Equation 7 in pH-units while Table 1 provides β -values from Equation 7 in units of $(HR)^{-1}$; why is there such a change ~every two weeks?
- (2) The magnitude of ΔpH ~doubles when temperature oscillations are present; what is this telling us?
- (3) The electrode-recalibration step with buffer solutions appears to shift the potential point back to the U(1) gauge value (see Table 1) so this clearly resets the electrode for the next 2 week run; but why is there such a change run to run?

Figure 7 teaches us that measurement sites that are underground, even with no IHDs present, can display significantly larger ΔpH -values than ground-level sites and even larger ΔpH -values than appreciably above ground-level sites⁽³⁾. Items 1 to 3 above brings to mind our general human experience with earthquake wave propagation wherein the wave amplitude increases in magnitude when it passes through a softer terrain and the wave velocity slows down. This suggest that, when considering intention-information entanglement mechanisms, one should not forget the concepts of (1) wave propagation through the R-space ground vs. R-space air, (2) R-space scattering events including feedback from location to location, (3) interface impedance mismatch with the particular pH-

measurement electrode being used and (4) the onset of appreciably higher frequency R-space wave propagation. Let us now consider Figure 8 and Poisson's Equation re relatively slow movement of electric charge as a possible rationale for explaining the Figure 7 behavior.

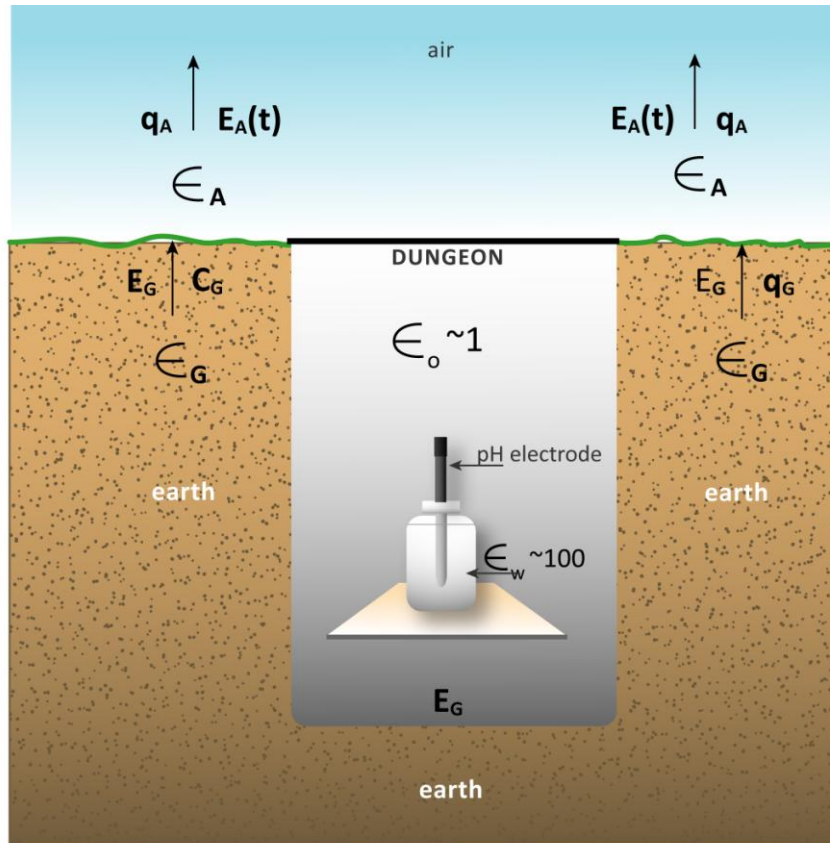


Figure 8. Illustration of Dungeon setup

From the Gauss' Law, the electric flux density, D , integrated over a closed surface equals the electric charge, ρ , enclosed. Maxwell converted this to

$$\nabla \cdot \underline{D} = \rho. \quad (8a)$$

Since $\underline{D} = \epsilon \underline{E}$ and $\underline{E} = -\nabla V$, where $\epsilon =$ the dielectric constant, \underline{E} is the electric field and V is the voltage, we have

$$\underline{D} = -\epsilon \nabla V \quad (8b)$$

Placing Equation 8b into 8a yields

$$\nabla \cdot \nabla V = -\rho / \epsilon \quad (8c)$$

or Poisson's Equation which can also be written as

$$\nabla^2 V = -\rho / \epsilon \quad (8d)$$

Returning our attention to Figure 8, the pH-measuring apparatus was on a table top about 3-4 feet above the floor of the room and deeply imbedded in the electric flux lines determined by the dielectric constant, ϵ_G , of the ground instead of that associated with the air, ϵ_A . If, for the moment, we neglect free charges in both the air and the ground, continuity of electric flux at the air/ground interface require that

$$\epsilon_A \underline{E}_A(t) = \epsilon_G \underline{E}_G(t) \quad (9a)$$

Since ϵ_G is very heterogeneous and is generally much greater than ϵ_A , it means that the electric fields normal to the earth are significantly larger in the air than in the ground. This would cause **electric shielding lengths**, λ , from free electric charge concentrations in the ground to be significantly larger in the ground than in the air. Thus, if one considers the effects of free charges in the environment **outside of the pH-electrode/water-bottle system** on the registered pH-measurement, the magnitude of the effect is significantly greater in the ground than in the air. Taking the earth's rotation in the solar radiation field into account, one can readily see the diurnal upper atmosphere ionization/recombination pattern moving laterally across the planet. This also drags an earth ion pattern both outwards to the

surface and inwards towards the planet's interior as well as laterally as the earth rotates. All of this requires that the electric flux continuity condition be written as

$$\epsilon_A \underline{E}_A(t) + q_A(t) = \epsilon_G \underline{E}_G(t) + q_G(t). \quad (9b)$$

The simultaneous solution to the second-order distance-time differential equations for D_A and D_G are ultimately needed to resolve the field, charge and current patterns in these two materials. For our purposes, here, we need only note that the pH-electrode in its water bottle will respond to this changing **outer** environment significantly more when the sensor monitoring it at a below ground site than at above ground sites. As an approximation to the general mathematical solution, at least in the ground, Equations 8 can be utilized with ρ and ϵ being slowly varying functions of time.

An Experimental Test Via a Negative-Ion Generator

In mid-May, 2011, using a ~5 foot cube-shaped, mu-metal coated box (Site P<7) as a controlled EM environment, a complete pH-measurement set-up and a negative-ion generator were arranged within a lateral separation distance of about 9 inches (see Figure 9).

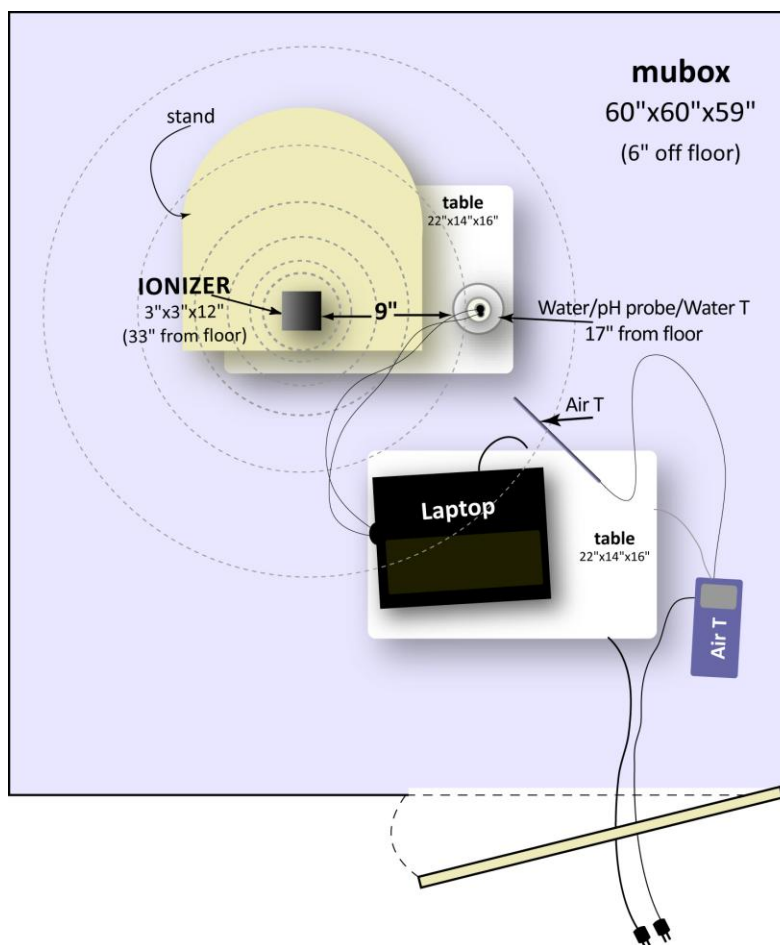


Figure 9. Floor diagram of mu-metal box with ionizer setup inside.

The ionizer was turned on May 19 and negative ions (electrons) began to populate this space at that time. Figure 10 clearly shows that this drove the measured pH downwards (more acidic) confirming the general nature of the previous section.

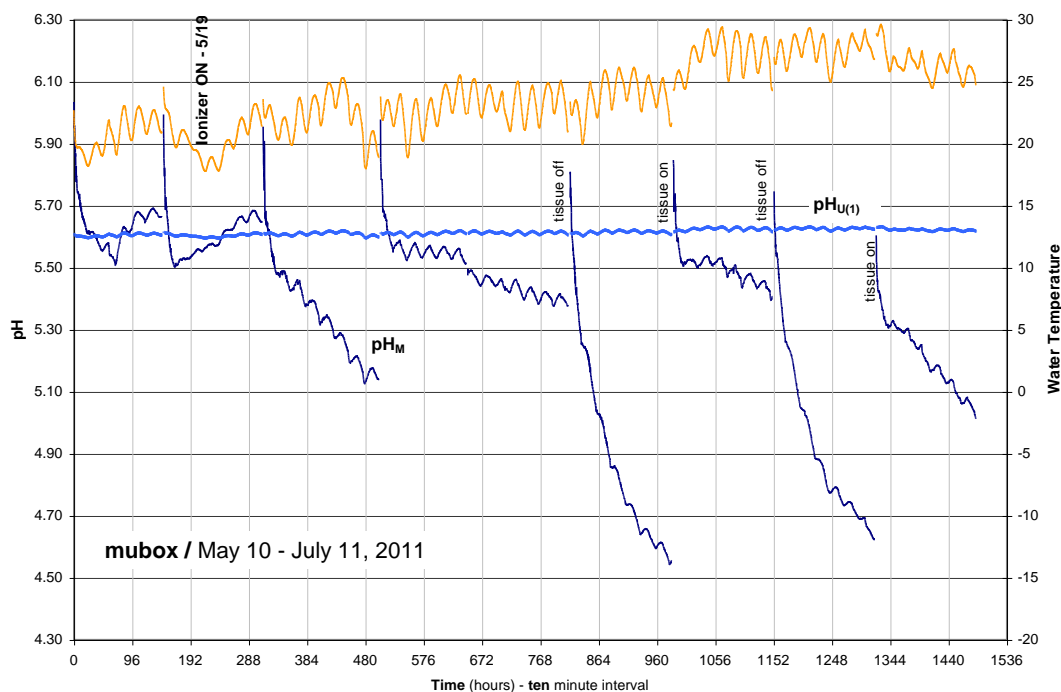


Figure 10. pH and temperature vs. time.

When the tissue paper was left off the top of the water bottle, between each recalibration cycle, the pH decreased more rapidly and to a greater extent. This result suggests that the negative ions did not enter the water and neutralize H^+ -ions but rather produced a surface polarization effect to either the outside surface of the bottle or to the free surface of the water which, in turn, drove the internal dissociation reaction in such a direction as to create more H^+ -ions.

Conclusions

1. A pH-measurement system can be effectively utilized to continuously monitor the excess thermodynamic free energy of the aqueous H^+ -ion during “space conditioning” from our normal U(1) EM gauge symmetry state to a higher EM gauge symmetry state via use of an imprinted IHD.
2. To enhance the absolute reliability of such measurements in a dynamically changing external EM environment, an EM screen and mu-metal screen will be needed to shield the water bottle and pH-electrode system.

References

1. W. A. Tiller, W. E. Dibble, Jr., and M. J. Kohane, Conscious Acts of Creation: The Emergence of a New Physics (Pavior Publishing, Walnut Creek, California, 2001).
2. W. A. Tiller, W. E. Dibble, Jr., and J. G. Fandel, Some Science Adventures with Real Magic (Pavior Publishing, Walnut Creek, California, 2005).
3. W. A. Tiller, Psychoenergetic Science: A Second Copernican-Scale Revolution (Pavior Publishing, Walnut Creek, California, 2007).
4. W.A. Tiller, and W. E Dibble, Jr., “New experimental data revealing an unexpected dimension to materials science and engineering”, *Mat. Res. Innovat.* (2001) 5:21–34.
5. W. A. Tiller and W. E. Dibble, Jr., “Toward General Experimentation and Discovery in Conditioned Laboratory and Complementary and Alternative Medicine Spaces: Part V, Data on 10 Different sites using a robust new type of subtle energy detector”, *JACM* 13 (1), 2007, pp 133-149.
6. W.A. Tiller & W.E. Dibble, Jr., “Towards understanding the internal symmetries of nature: Gauge symmetry states”, Free White Paper XIX, www.tiller.org.
7. K. Moriyasu, An Elementary Primer for Gauge Theory, (World Scientific Publishing Co. PTE. Ltd. Singapore, 1983).
8. W.A. Tiller Ph.D., W.E. Dibble, Jr. Ph.D., and T. Ludwig Ph.D., “Towards understanding long-range broadcasting of specific intentions”(submitted for publication to *The Journal of Scientific Exploration*, June 2011).
9. W.A. Tiller, and W. E Dibble, Jr., “Steps for moving psychoenergetic science research into the hands of interested general public researchers”, Free White Paper II, www.tiller.org.
10. K. Moriyasu, An Elementary Primer for Gauge Theory (World Scientific Publishing Co. PTE. Ltd. Singapore, 1983).

11. W.A. Tiller & W.E. Dibble, Jr., “Towards understanding the internal symmetries of nature: Gauge symmetry states”, Free White Paper XIX, www.tiller.org.
12. W.A. Tiller, and W. E Dibble, Jr., “An experimental investigation of some Reconnective healing workshops via a unique subtle energy detector”, Free White Paper XI, www.tiller.org.